Reinforcement of macroscopic carbon nanotube structures by polymer intercalation: The role of polymer molecular weight and chain conformation

C. J. Frizzell

Department of Physics & NanoTech Institute, The University of Texas at Dallas, 2601 N. Floyd Rd., Richardson, Texas 75083, USA
and Department of Physics, Trinity College Dublin, Dublin 2, Ireland

M. in het Panhuis*

Department of Physics & NanoTech Institute, The University of Texas at Dallas, 2601 N. Floyd Rd., Richardson, Texas 75083, USA
and Department of Physical Sciences, the University of Hull, Hull, HU6 7RX, United Kingdom

D. H. Coutinho and K. J. Balkus, Jr.

Department of Chemistry, The University of Texas at Dallas, 2601 N. Floyd Rd., Richardson, Texas 75083, USA

A. I. Minett, W. J. Blau, and J. N. Coleman

Department of Physics, Trinity College Dublin, Dublin 2, Ireland

Novel polymer nanotube composites were fabricated by intercalating poly(vinylpyrrolidone) into Buckypaper from solution. This was carried out for both low ($10k$ g/mol) and very high ($1.3M$ g/mol) molecular weight polymers. Measurements of the polymer mass uptake as a function of time allowed the calculation of diffusion coefficients as 1.66×10^{-9} cm²/s and 3.08×10^{-12} cm²/s for the low and high molecular weight strands, respectively. Taking into account the molecular weights, comparison of these coefficients suggests that each polymer type undergoes a different mode of diffusion: normal diffusion for the $10k$ g/mol polymer, but reptation for the $1.3M$ g/mol polymer. This means that while the low weight polymer retains its randomly coiled conformation during diffusion and adsorption, the $1.3M$ g/mol molecule is forced to adopt an extended, high entropy state. These differences are reflected in the mechanical properties of the intercalated papers. While reinforcement was observed in all cases, modulus (increase $\sim \times 3.5$) and strength (increase $\sim \times 6$) enhancement occurred at lower polymer content for the longer chain polymer. However, the papers intercalated with the shorter chain molecules were much tougher (increase $\sim \times 25$). This is consistent with the conformation scheme described above.

PACS number(s): 81.07.De, 62.25.+g, 81.05.Qk

I. INTRODUCTION

Single-walled carbon nanotubes (SWNT) are a remarkable material with superb mechanical properties. Exceptional values of up to 1500 GPa for Young's modulus[1] and ~50 GPa for tensile strength[2] have been demonstrated. However, potential macroscale applications have been hindered as bulk nanotube material consists mainly of aggregated bundles bound together by weak van der Waals interactions. This results in a massive reduction in the bulk mechanical properties when compared to that of individual tubes. Recently, some progress has been made using polymer solution based processing to organize nanotube containing powder into functional macroscale composite materials in the form of fibers[3] and films.[3–5] However, these improvements in nanotube based material properties rely on dispersing nanotubes in a polymer based matrix.

In previous work[6] it was shown that the reverse procedure of polymer intercalation can be used to reinforce bulk nanotube materials. The mechanical properties of as-prepared (pristine) sheets of carbon nanotubes (Buckypaper) were significantly improved by soaking the sheets in various organic polymer solutions. Increases of approximately ×3 in Young's modulus and ×9 in tensile strength were obtained.

This work is important as polymer intercalation (either *in situ* or postproduction) is required to maximize both the strength and toughness of high performance nanotube fibers.[3] However, questions such as the intercalation mechanism and the role of molecular weight remained unanswered.

In this paper, we use carbon nanotube sheets (Buckypaper) as a model system to examine the reinforcement effects of polymer intercalation on macroscale nanotube structures. The effects of soaking Buckypaper in organic polymer solutions of poly(vinylpyrrolidone) (PVP) are investigated. Studies of polymer intercalation as a function of time for two molecular weights demonstrate the diffusion mechanisms for low and high molecular weight polymers. Mechanical studies show that reinforcement is significantly more efficient for the high molecular weight polymer. This is shown to be related to the polymer conformation during the diffusion and subsequent adsorption process.

II. EXPERIMENTAL DETAILS

Carbon nanotube sheets (Buckypaper) were made by dispersion of HiPco SWNT (Carbon Nanotechnologies, Inc., HiPco Bucky Pearls™ batch no. P0-185)[7] in aqueous solutions of Triton X-100. Single-walled carbon nanotubes are
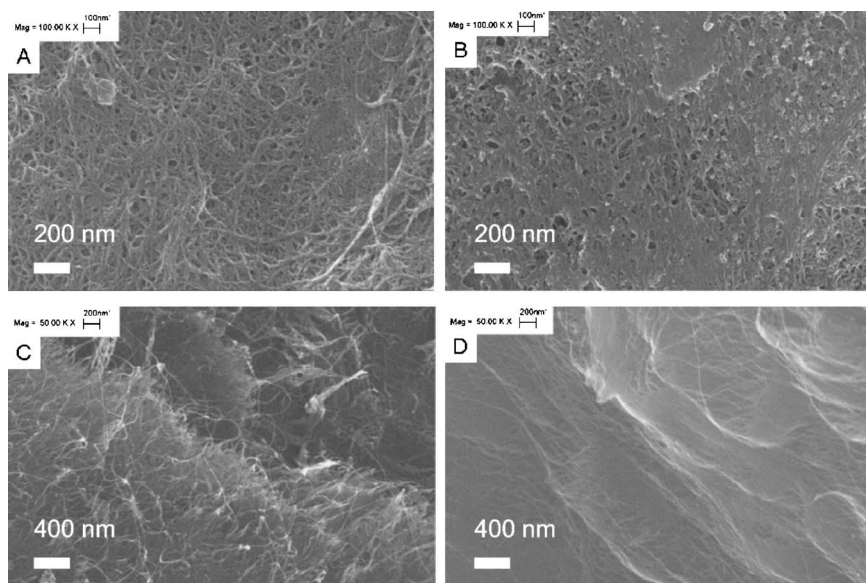
FIG. 1. Scanning electron micrograph images of typical reference (pristine) and polymer soaked Buckypaper. (a) Surface and (c) cross section of reference paper. (b) Surface and (d) cross section of paper soaked in PVP (10 000 g/mol) solution for 12 h.

produced by the high pressure decomposition of carbon monoxide in the presence of an iron catalyst (indicated by the acronym HiPco).[7] Dispersions were prepared by mixing 180 mg of HiPco SWNT in 0.5% (wt/vol) aqueous solutions of Triton X-100, using a combination of low power (bath) and high power (tip) sonication. These dispersions were then vacuum filtered through Millipore Mitex PTFE membrane filters (pore size=5 μm, diameter=90 mm). The resulting nanotube sheets were washed with 5 L water, followed by washing with ethanol until the foam disappeared, indicating that the majority of the surfactant had been removed. Subsequently, the sheets were allowed to dry under vacuum for 12 h. The as-prepared (pristine) sheets were then cut into rectangular strips of $\approx$2 mm $\times$ $\approx$20 mm $\times$ $\approx$60 μm and annealed at 500 °C for 2 h under flowing argon to remove any residual surfactant and contaminants. Density measurements were made for each strip using a Whitworth digital caliper for width and length measurement, a Mitoutoyo micrometer for thickness measurements and a Mettler Toledo microbalance for mass measurements.

Aqueous solutions of 2.5% (wt/vol) PVP (an amphiphilic semiconjugated polymer) in deionized water were prepared using polymer molecular weights (M_w) of 10 000 and 1 300 000 g/mol. A number of Buckypaper strips were soaked in polymer solutions of both molecular weights for various soak times. For each M_w and soaktime, five strips were soaked. Soak times ranged from 10 min to 24 h for low molecular weight polymer and from 12 to 360 h for high molecular weight polymer. After soakage, all strips were carefully rinsed in deionized water and placed in a vacuum oven for 12 h at approximately 60 °C to remove residual water from the samples. Strip masses were measured a second time and any mass increase recorded. All reported mass increases are averages over five strips.

Tensile tests were carried out on all samples to determine Young's modulus, strength and toughness using a Perkin Elmer DMA7e. For all soak times, five strips were measured and the mean and standard deviation calculated. Scanning electron microscopy (SEM) images of various strips were

taken using a Leo 1530VP field emission SEM. Thermogravimetric analysis (TGA) was carried out to determine polymer mass percentage and catalyst content in the sheets using a Perkin Elmer Pyris TGA1 under an oxygen atmosphere (scan rate 10 K/min).

Nitrogen absorption and desorption experiments were carried out on annealed sheets. The results were analyzed using multiple theories such as the BET, BJH, and HK methods. The specific surface area is calculated (using BET method) from information about the amount of N_2 molecules absorbed on the surface and the surface area occupied by each molecule. The pore characteristics are calculated (using BJH and HK methods) from the fact that smaller pores will fill up quicker than the larger pores during absorption.

III. RESULTS AND DISCUSSION

After fabrication the Buckypaper strips resembled pieces of stiff matt black paper. Shown in Fig. 1(a) is an SEM image of the surface of a typical strip. It can be clearly seen that the surface of the material is made up of bundles of nanotubes with diameters ranging up to tens of nanometers. In addition a large number of pores can be seen indicating that the bundles pack together rather inefficiently. The pore sizes appear to be of the same order as the bundle diameters. Shown in Fig. 1(c) is an SEM image of a fracture surface allowing the investigation of the inside of the paper. It can be seen that the interior is characterized by substantial free volume again emphasizing the inefficient nature of the bundle packing. This is underlined by the low density of the material which was measured to be $\rho_{paper}=520\pm100$ kg/m^3. The interbundle fractional free volume (V_f/V_T) can be calculated from the density by $V_f/V_T=1-\rho_{paper}/\rho_{NT}$, where ρ_{NT} is the nanotube bundle density which can be estimated as 1500 kg/m^3 (Ref. 6). This results in an interbundle free volume of $V_f/V_T=66\pm7$% meaning that the material is dominated by the pores.

To investigate this further, N_2 adsorption/desorption isotherms were measured for the annealed Bucky paper. This
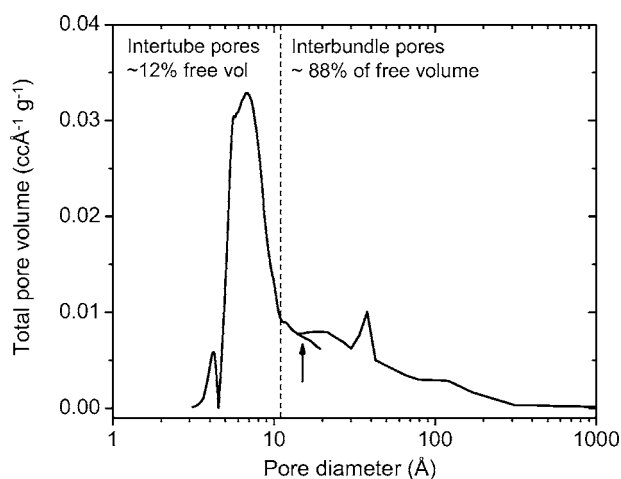
FIG. 2. Pore size distribution for annealed Buckypaper measured from N_2 adsorption-desorption isotherms. Pore sizes of <2 nm were calculated by the HK method while those of >2 nm were calculated using the BJH method. The point where the data sets were joined is shown by the arrow where a small mismatch can be seen. The peak around 6 Å is associated with internanotube pores; that is, the channels between nanotubes within bundles. The upper limit of this region is marked by the dotted line. The region of the graph to the right of the dotted line represents the interbundle pores.

data could then be used to calculate the pore size distribution within the sheet. This is carried out using the Horvath-Kawazoe[8] (HK) method to calculate small-diameter pore sizes (<2 nm) and the Barrett, Joyner, and Halenda (BJH) method[9] to calculate the size of larger pores (>2 nm). Both methods gave results that agreed well in the crossover region around 2 nm. Both data sets have been combined and are shown in Fig. 2. The crossover region is indicated by the arrow. The data is dominated by a large peak between 4 and 11 Å. These relatively small pores are associated with the channels between nanotubes within bundles and can be thought of as interstitial pores. It should be noted that as the nanotubes are capped, the internal channels are not accessible to either gas adsorption or molecular intercalation. For trigonal packing within bundles, the interstitial pore size as a function of nanotube diameter can be easily calculated.[10] This shows that the upper limit of the distribution of smaller pores shown in Fig. 1 occurs for bundles of nanotubes with diameter ~ 1.3 nm. This is close to the upper end of the diameter range for HiPco nanotubes.[11] Numerical integration shows that these intertube pores contribute $\sim 12\%$ of the total free volume of the Buckypaper. However, the pores with diameter larger than 11 Å are associated with the space between bundles. It is these interbundle pores that are observed in the SEM images. The distribution displays peaks at approximately 4 nm and a long tail out to 100 nm. As they contribute $\sim 88\%$ of the total free volume, the presence of these pores will have a significant impact on the physical properties of the paper as a whole.

In addition, multipoint Brunauer, Emmett, and Teller[12] (BET) analysis was used to calculate the specific surface area, A_S, of the paper. This was calculated as $A_S=611$ m^2/g

which is slightly larger than previous reports.[13] By neglecting the contribution due to the intertube pores A_S can be used to approximate the bundle diameter. Assuming that A_S is simply due to the outer surface of a large number of bundles with diameter, D_{bun}, then A_S can be expressed as $A_S=4/\rho_{NT}D_{bun}$, yielding $D_{bun}=4.5$ nm. However, this value is rather small and should be considered a lower limit.

In partial summary, the Buckypaper can be considered an amalgam of randomly ordered nanotube bundles with diameters ranging from a few nanometers to a few tens of nanometers. Between these loosely packed bundles is empty space which makes up 60—70 % of the volume of the paper. This free volume consists of pores with sizes ranging from one to hundreds of nanometers. In short this material should be well suited for the intercalation of polymeric material.

In order to study the intercalation of polymers into the free volume discussed above, sheets of Buckypaper were soaked for various times in solutions of PVP of two different molecular weights. After soaking the sheets were rinsed and dried before weighing to measure polymer mass uptake. In all cases significant mass uptake was observed. To check that this did not just consist of a surface coating, SEM studies were carried out. Shown in Fig. 1(b) is an SEM image of a Buckypaper strip after soaking for 12 h on PVP with M_w $=10\,000$ g/mol. By comparison with Fig. 1(a) it can clearly be seen that a layer of polymer has coated the surface of the sheet. However, as the pores are still visible this layer cannot be very thick, suggesting that the majority of the mass uptake is associated with intercalated polymer. To confirm this, an SEM image was taken of a fracture surface allowing us to image the interior of the sheet. This is shown in Fig. 1(d) and clearly shows that the polymer has intercalated far into the bulk of the paper. In fact no regions were observed corresponding to Fig. 1(c) indicating that the intercalated polymer had covered the entire internal surface of the paper. Similar results were obtained for the $M_w=1.3M$ g/mol PVP (not shown). This shows clearly that the polymer macromolecules can diffuse very long distances into the paper before adsorbing onto the internal surface of the paper.

To understand the diffusion process the mass of intercalated polymer, termed the mass uptake, was measured for a number of soak times for each molecular weight. This is shown in Figs. 3(a) and 3(b) as the intercalated polymer mass (m_P) normalized to the mass of the paper before intercalation (m_{NT}). For the low molecular weight polymer the mass uptake rises very rapidly before saturating after 1 h at 30—40 % of the initial paper mass. However for the high molecular weight the increase is much more gradual, reaching 14% of the original paper mass after 360 hours with no sign of saturation.

As we know the specific surface area of the paper, A_S, it is possible to transform (m_P/m_{NT}) to represent the fraction of internal surface area covered by polymer, θ_C. If we assume that the maximum coating thickness is one molecular layer then the fractional coverage can be expressed by

$$\theta_C = \left(\frac{m_P}{m_{NT}}\right)\frac{1}{A_S\rho_P h},\tag{1}$$

where ρ_P is the polymer density ($\rho_P=1660$ kg/m^3) and h is the polymer film thickness, i.e., the molecular size. As we
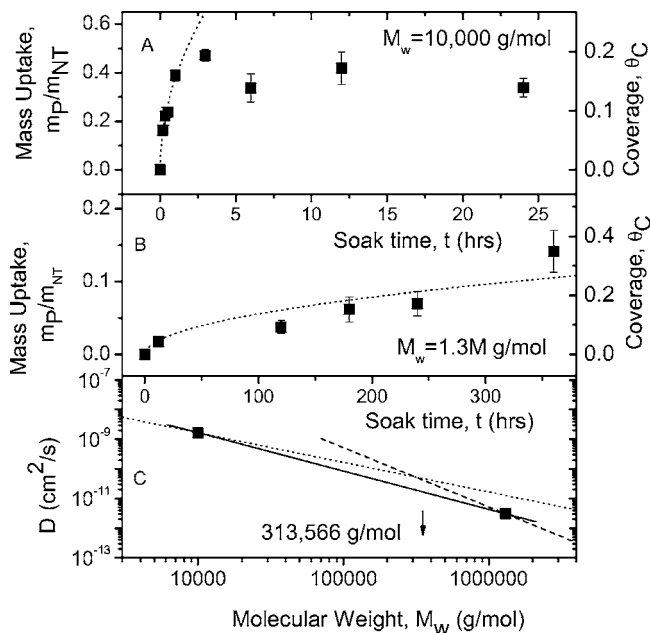
FIG. 3. (a) Polymer mass uptake as a function of soak time for PVP with $M_w=10\,000$ g/mol. The dotted line is a fit to Eq. (2) with $D=1.66\times10^{-9}$ cm^2/s and $l=60$ μm. Note that the intercalation saturates after approximately 1 h. (b) Polymer mass uptake as a function of soak time for PVP with $M_w=1.3M$ g/mol. The dotted line is a fit to Eq. (2) with $D=3.08\times10^{-12}$ cm^2/s and $l=60$ μm. In this case there is no sign of saturation even after 360 h. In both (a) and (b) the fraction of the internal surface coated by the polymer is shown as the right axis as calculated by Eq. (1). (c) Diffusion coefficients calculated from Figs. 3(a) and 3(b) as a function of M_w. The solid line is a fit to $D_M \propto M_w^{-n}$, giving $n=1.29$. Rouse diffusion ($n=1$) is depicted by the dotted line while reptation ($n=2$) is illustrated by the dashed line. The intersection of these two regimes occurs at $M_w=313\,566$ g/mol.

shall see below, it is very likely that the low M_w polymer adsorbs as a random coil. The molecular size and hence the film thickness (h) can be estimated as the root mean square radius of the coil ($R_{rms}=\sqrt{6}\times R_g$),[14] $R_{rms}=2.4$ nm~h. Again, as we shall see later, the $M_w=1.3$ Mg/mol polymer adsorbs in an extended state so we can estimate h as close to the molecular thickness, i.e., slightly larger than the van der Waals distance, $h\sim 0.4$ nm. Using these values, and noting that the specific surface area of the pristine paper is 611 m^2/g, we can calculate the fractional surface coverage, θ_C, as a function of soak time for both molecular weights. This is shown as the right axis in Fig. 3. We can clearly see that the mass uptake saturates for fractional coverage range 15—20 % for the low M_w polymer but is still increasing for fractional coverage of 35% for the high M_w polymer.

The pores present in the Buckypaper can be considered as long highly branched channels of extremely irregular cross section. In general, diffusion can be characterized by an average displacement from the starting point, $\langle x \rangle$, that varies in time, t, as $\langle x \rangle \sim (Dt)^{1/2}$ where D is the diffusion coefficient.[14] Similarly, Fickian mass transport of molecules into porous materials by diffusion displays similar temporal behavior with a square root time dependence.[15] In this case, the inter-

calated mass uptake as a function of time is given by[16]

$$\frac{m_P}{m_{NT}} = \left(\frac{m_P}{m_{NT}}\right)_{sat} \sqrt{\left(\frac{16D}{b^2\pi}\right)}t, \qquad (2)$$

where $(m_P/m_{NT})_{sat}$ is the saturated value of the mass uptake, D is the diffusion coefficient, and b is the film thickness.

Equation (2) was fitted to the data in Figs. 3(a) and 3(b) taking $b=60$ μm. In both cases the fit was reasonably good, indicating the validity of Eq. (2). The fitting routine gave values of D of 1.66×10^{-9} cm^2/s and 3.08×10^{-12} cm^2/s for the 10 000 g/mol and 1.3M g/mol polymers, respectively. These values are in the range expected for macromolecules confined within porous media.[15] As one would imagine the diffusion constant for the higher molecular weight polymer is much lower compared to that for the $M_w=10\,000$ g/mol case.

The time scale for diffusion of a polymer in a porous medium depends on the size of the polymer molecule compared to the pore size, d. When the radius of gyration, R_g, of the polymer is much less than the pore size ($R_g \ll d$) the polymer does not feel the strong topological constraints imposed by the pore walls and so can diffuse normally. Here the Rouse diffusion model is appropriate[17–19] and $D \propto M_w^{-1}$. In this situation the polymer retains its high entropy, randomly coiled state. However in the opposite regime when, $R_g \gg d$, the strong topological constraints imposed by the pore walls dominate and motion along the polymer's contour is much more favorable. This is known as reptation[18–20] and is characterized by $D \propto M_w^{-2}$ (Ref. 21).

The radius of gyration of a polymer chain is given by $R_g=l(N/6)^{1/2}$, where N is the number of repeat units and l is the repeat unit length.[14,18] Given that the length of the PVP repeat unit is ~ 0.25 nm and its mass is 111.14 g/mol we can calculate R_g as ~ 0.97 nm and ~ 11.0 nm for the low and high molecular weight polymers, respectively. As the pore size distribution peaks at 4 nm (Fig. 2) we might expect the $M_w=10\,000$ g/mol polymer to diffuse according to the Rouse model and the $M_w=1.3M$ g/mol polymer to move by reptation. We can test this by plotting D versus M_w for both polymers and fitting to $D \propto M_w^{-n}$. This is shown in Fig. 3(c) where the solid line represents the fit with $n=1.29$. The fact that $1<n<2$ suggests that the two molecular weights diffuse according to the different models as suggested above. The dependence of D on M_w is plotted as a dotted line for the Rouse model and as the dashed line for reptation. The crossover between these two regimes, as identified by the intersection of these lines, should occur for an M_w corresponding to a polymer radius of gyration that matches the average pore size $\langle d \rangle$.[19] This crossover occurs at $M_w=313\,566$ g/mol which corresponds to $R_g=5.4$ nm. This is in excellent agreement with the peak in the pore size distribution which occurs at $d=4$ nm.

This result is important as it means that the $M_w=10\,000$ g/mol polymer diffuses through the Buckypaper as a randomly coiled chain. However, topological constraints mean that the 1.3M g/mol polymer is forced to unravel and move along its contour in an extended conformation. Furthermore when a given chain eventually adsorbs into the
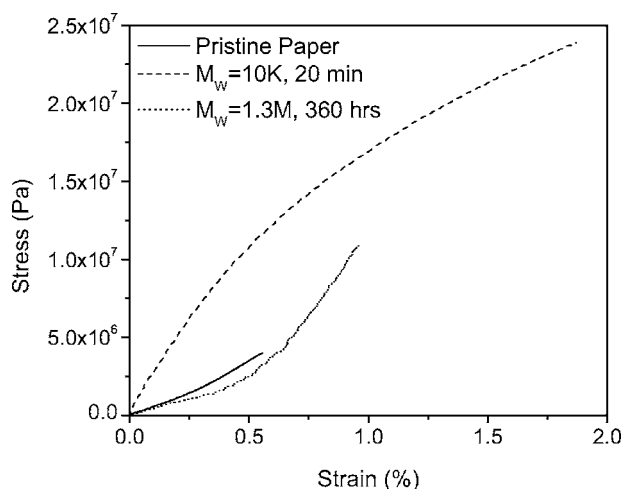
FIG. 4. Representative stress strain curves for the pristine paper, paper soaked in PVP with $M_w = 10\,000$ g/mol, and paper soaked in PVP with $M_w = 1.3M$ g/mol. Note that no individual stress strain curve displayed the average behavior for modulus, strength, *and* toughness. These curves were chosen to illustrate the general shape of the stress strain curves and their relative toughness'.

internal surface of the paper it is likely that it retains approximately its conformation while diffusing. This means that the intercalated polymer chains exist in very different confirmations for low and high molecular weight polymers. This is expected to have a significant effect on the physical properties of the polymer intercalated Buckypaper.

For both molecular weights, mechanical measurements, in the form of stress-strain curves were carried out as a function of mass uptake. Three typical curves for the pristine, annealed paper, paper soaked with $M_w = 10\,000$ g/mol for 20 minutes and paper soaked with $M_w = 1.3M$ g/mol for 360 hours are shown in Fig. 4. All curves displayed a linear region at low strain followed by plastic deformation above a strain of ~0.3%. Fracture was observed at strains of approximately 0.5%, 1.0%, and 1.8% for the pristine paper, the 1.3M g/mol intercalated paper and the 10 000 g/mol intercalated papers, respectively. For all stress-strain curves the Young's modulus, Y (slope at low strain), the ultimate tensile strength, σ_B, (stress at break), and toughness, T, (area under curve, energy per unit volume required to break) were calculated. These parameters are plotted for high and low molecular weights in Figs. 5 and 6, respectively, as a function of volume fraction, V_f. In all cases mass uptake was transformed into volume fraction using Eq. (3):

$$V_f = \left[1 + \left(\frac{\rho_P}{\rho_{NT}} \right) \left(\frac{m_{NT}}{m_P} \right) \right]^{-1}, \tag{3}$$

where ρ_P and ρ_{NT} are the polymer and nanotube mass densities respectively ($\rho_P = 1660$ kg/m³, $\rho_{NT} = 1,500$ kg/m³). All the relevant parameters quoted in the next paragraph are given in Table I. (NB a different sheet of Buckypaper was used for each molecular weight intercalation study. Each sheet had slightly different mechanical properties. These are presented at the top of Table I.)
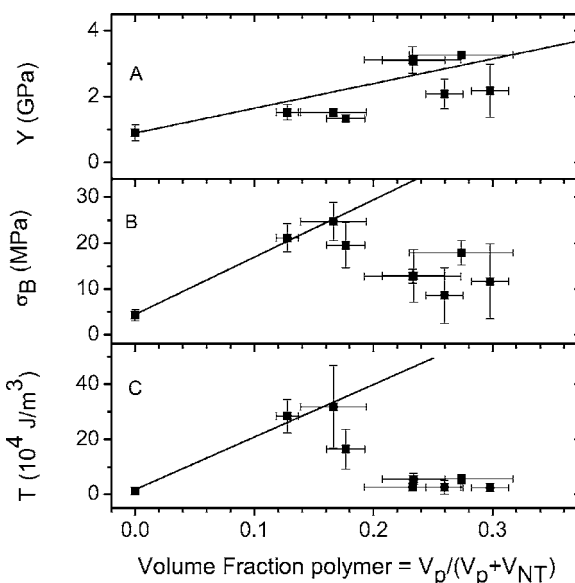

FIG. 5. Mechanical properties of Buckypaper intercalated with PVP of $M_w = 10\,000$ g/mol. (a) Young's modulus, Y, as a function of volume fraction. The line is a fit to Eq. (4) with $dY/dV_f = 7.49$ GPa. (b) Ultimate tensile strength, σ_B, as a function of volume fraction. At low volume fraction the data is linear with slope $d\sigma_B/dV_f = 125$ MPa. However, σ_B tends to drop off above $V_f = 0.17$. (c) Toughness, T, as a function of volume fraction. At low volume fraction the data is linear with slope $dT/dV_f = 1.91$ MJ/m³. However, T tends to drop off above $V_f = 0.17$.

For the paper intercalated with the low molecular weight polymer (Fig. 5) the Young's modulus increases approximately linearly with a slope of $dY/dV_f = 7.49$ GPa before attaining a maximum value of $Y_{max} = 3.3$ GPa representing an increase over the pristine paper of ×3.6. In comparison, the high molecular weight polymer (Fig. 6) displays a linear increase in Young's modulus ($dY/dV_f = 57.5$ GPa) at low volume fraction before saturating at $V_f = 0.03$. The maximum modulus attained was $Y_{max} = 3.16$ GPa which was an increase of ×3.7.

While the maximum values of Young's modulus attained are similar and agree with previous results[6] the dY/dV_f values display a marked difference between molecular weights. Generally, the Young's modulus of composites are analyzed using the so-called rule of mixtures[5,22] which states that for a mixture of components 1 and 2, the resultant modulus, Y, is given by

$$Y = (Y_1 - Y_2)V_f + Y_2, \tag{4}$$

where V_f is the volume fraction of phase 1. In our case, treating the polymer as phase 1, and using equation (4), the measured dY/dV_f values give polymer moduli of 8.4 GPa and 58.4 GPa for the low and high molecular weight polymers, respectively. These values are much too large to be realistic as typical non-conjugated polymers such as poly(vinylalcohol) and poly(styrene) have moduli in the 0.2–4 GPa range.[23] The fact that these values are too large suggests that the reinforcement mechanism is not one of typical mixing.
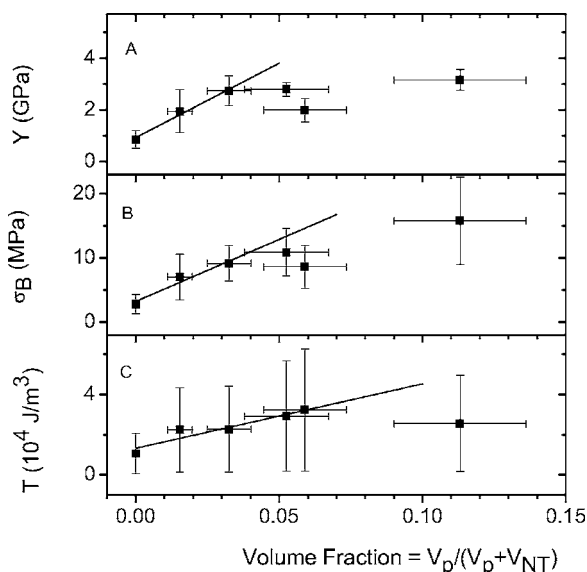
FIG. 6. Mechanical properties of Buckypaper intercalated with PVP of $M_w=1.3M$ g/mol. (a) Young's modulus, Y, as a function of volume fraction. The line is a fit to Eq. (4) with $dY/dV_f=57.5$ GPa. However, Y tends to saturate above $V_f=0.04$. (b) Ultimate tensile strength, σ_B, as a function of volume fraction. At low volume fraction the data is linear with slope $d\sigma_B/dV_f=193$ MPa. However, σ_B tends to saturate above $V_f=0.04$. (c) Toughness, T, as a function of volume fraction. At low volume fraction the data is linear with slope $dt/dV_f=321$ kJ/m³. However, T tends to saturate above $V_f=0.04$.

In the case of ultimate tensile strength the picture is similar. For the paper intercalated with the low molecular weight polymer (Fig. 5) the strength increases approximately linearly with a slope of $d\sigma_B/dV_f=125$ MPa before reaching a maximum value of $\sigma_{B,max}=24.7$ MPa (increase: ×5.8) at a volume fraction of 0.17. Above this volume fraction the strength drops off. In comparison, the high molecular weight polymer (Fig. 6) also displays a linear increase in strength ($d\sigma_B/dV_f=193$ MPa) at low volume fraction before saturating at $V_f=0.03$. The maximum strength attained was $\sigma_{B,max}=15.8$ MPa which represents an increase of ×5.6. Again, in both cases the increase in strength compared to the pristine Buckypaper was similar while $d\sigma_B/dV_f$ was significantly larger for the higher molecular weight polymer. As in the case with the modulus, these results cannot be explained by the intrinsic strength of the polymers themselves.

Finally, the toughness results are in contrast to those for the modulus and strength. For the paper intercalated with the low molecular weight polymer (Fig. 5) the toughness also increases approximately linearly with a slope of $dT/dV_f=191$ J/m³ before reaching a maximum value of $T=31.8 \times 10^4$ J/m³ (increase: ×26) at a volume fraction of 0.17. Above this volume fraction the toughness drops off. However, the high molecular weight polymer (Fig. 6) also displays a linear increase in toughness but with a much lower slope ($dT/dV_f=32.1$ J/m³) at low volume fraction before saturating at $V_f=0.03$. In this case the maximum toughness was only $T=3.23 \times 10^4$ J/m³ which represents an increase of only ×3.0. This raises the question: why do strength and

TABLE I. Summary of values found in this study. Comparisons between absolute values of the maximum in mechanical properties may be misleading as a different sheet of Buckypaper was used for each molecular weight intercalation study. Each sheet had slightly different properties. These are presented at the top of the table. A more reliable value is the maximum relative increase in properties. This is shown in brackets.

	$M_w=10\,000$ g/mol	$M_w=1.3M$ g/mol
Y_{NT} (GPa)	0.903	0.857
σ_{NT} (MPa)	4.29	2.8
T_{NT} (J/m³)	1.22	1.06
$(m_P/m_{NT})_{max}$	0.47	0.14
D (cm²/s)	1.66×10^{-9}	3.08×10^{-12}
$Y_{C,max}$ (GPa)	3.26 (×3.6)	3.16 (×3.7)
dY_C/dV_f	7.49	57.4
$\sigma_{C,max}$ (MPa)	24.7 (×5.8)	15.8 (×5.6)
$d\sigma_C/dV_f$ (MPa)	125	193
$T_{C,max}$ ($10^4 \times$ J/m³)	31.8 (×26)	3.23 (×3.0)
dT_C/dV_f (J/m³)	191	32.1

modulus increase more efficiently for the high M_w intercalant but toughness displays the opposite behavior?

This question can be answered by examining both the fractional surface coverage and conformations of the two types of intercalated polymers. As shown in Figs. 5 and 6, both strength and toughness saturate at volume fractions, V_f (m_P/m_{NT}) of 0.17 (0.23) and 0.03 (0.037) for the low and high molecular weights, respectively. Using Eq. (1), we can calculate the fractional surface coverage, θ_C, as ~9% for both molecular weights at saturation. Thus taking the conformation into account, the fractional surface coverage over the linear regime is similar for both polymers. Thus variations in fractional surface coverage cannot explain the differences in mechanical properties.

This means that the differences must lie in the polymer conformations rather than in surface coverage. We have shown that the mechanism of reinforcement is not that of simple mixing. One other possibility is that the intercalated polymer acts as a binder which enhances the interbundle adhesion as suggested previously.[6] As noted above, the low M_w polymer adsorbs in the coiled conformation. This would tend to act as a rather localized, inefficient binder, connecting no more than two bundles per molecule. In contrast the high molecular weight polymer adsorbs in an extended conformation which has a contour length of approximately 3 µm ($=Nl$). These extended strands act to bind a large number of bundles together acting as a very efficient binder. This would result in more efficient enhancement of both strength and modulus for the paper intercalated with the high molecular weight polymer.

This model also explains why the toughness is higher for the low M_w material. When a stress is applied, a large amount of work must be done to unravel and finally separate two bundles initially bound by a low M_w, randomly coiled strand. This is because it requires a significant energy input

to go from a high entropy, coiled state to a low entropy, extended state. This results in a relatively high toughness. This is a similar mechanism to that which gives rubber its elasticity.[24] However for the high M_w polymer, as it is already extended, there is little scope to unravel it on application of a stress resulting in lower toughness.

We can very crudely estimate the potential of this method for toughness enhancement. The contribution to the toughness per polymer strand from the work required to unravel the coil is given by the free energy increase, $\Delta G = -T\Delta S$, where ΔS is the increase in entropy associated with going from a coiled to an extended state. This can be approximated, for a uniaxial force by[25]

$$\Delta S \sim -\frac{k}{2}\lambda^2, \qquad (5)$$

where k is Boltzmann's constant and λ is the chain extension ratio. This can be approximated as the ratio of the chain end to end separation before extension to that after. The average end-to-end separation for a random coil is $R_{rms} = l\sqrt{N}$ (the symbols have the same meaning as before). If we assume complete extension, then the end-to-end length (contour length) afterwards is $\sim Nl$. This means that $\lambda = \sqrt{N}$, giving $\Delta G \sim \frac{1}{2}kTN$ per chain. The number of chains per volume is

$$N_{chain}/V = \left(\frac{m_P}{m_{NT}}\right)\frac{\rho_{paper}}{m_{chain}}, \qquad (6)$$

where m_{chain} is the mass of each polymer chain. This means that the toughness (or work done per unit volume) can be expressed as

$$T = \frac{kTN}{2}\left(\frac{m_P}{m_{NT}}\right)\frac{\rho_{paper}}{m_{chain}}. \qquad (7)$$

For the 10 000 g/mol polymer at saturation ($m_P/m_{NT} = 0.23$) this yields a (calculated) toughness of $T = 1.33 \times 10^6$ J/m^3. This is within order of magnitude agreement with the measured toughness of $T \sim 3 \times 10^5$ J/m^3. We would expect the calculated value to be greater than the measured value as it is unlikely that the chains would fully unravel before film fracture. However, the agreement of even such a crude estimate with the measured value is encouraging and suggests that toughness can be tailored by control of the molecular weight. Indeed, the toughness could be maximized by intercalating the maximum possible molecular weight polymer that can still diffuse as a random coil. In the case of the Buckypaper used here, that would be for $M_w \sim 313\,566$ g/mol ($R_g \sim \langle d \rangle$).

This result is important as fibers fabricated from SWNT and poly(vinylalcohol) have been shown to be very strong and more importantly, among the toughest macro scale materials known to man.[3] However, the molecular weight of the polymer used for fiber production has yet to be optimized. In our work we have shown that in certain circumstances where polymer conformation is constrained during sample preparation, molecular weight can have a large bearing on the resultant mechanical properties. While high molecular weight polymer binders are important for strength enhancement, shorter chains can be used to enhance toughness. This would be particularly useful for example, as a postproduction treatment for directly spun nanotube fibers.[26,27] We believe that careful choice of molecular weight or even blending of two or more polymers of different molecular weights could result in further improvements in these already impressive fiber materials.

IV. CONCLUSION

In conclusion we have shown that SWNT Buckypaper contains a significant fraction (60–70 %) of free volume in the form of one-dimensional branched pores. These pores are characterized by a diameter distribution that varies from one to well over a hundred nanometers. An amphiphillic, non-conjugated polymer, such as PVP, could easily be intercalated into these pores simply by soaking the Buckypaper in polymer solutions at both low and very high molecular weights. By monitoring the intercalated mass uptake as a function of time, the polymer diffusion coefficient could be calculated for each molecular weight. Comparison of the diffusion coefficients as a function of M_w suggested that the low weight polymer diffuses normally through the pores while the larger polymer moves by reptation. This is significant as it means that the low and high molecular weight strands move as a random coil and in an extended state, respectively. As it is likely that this conformation will be, at least partially, retained on adsorption this will be significant for the properties of the resultant composite. Mechanical measurements show that Young's modulus, strength and toughness of the Buckypaper are all enhanced by polymer intercalation. However, enhancement of both modulus and strength is significantly more efficient for papers intercalated with the high molecular weight polymer. In contrast the opposite scenario is observed for toughness. This apparent paradox in mechanical properties can be explained by differences in polymer conformation ("coil" for low M_w and "extended chain" for high M_w polymer) and their ability to bind and unravel under applied stress. This underlines the importance of polymer confirmation for reinforcement in nanotube containing composites. This result could be used to significantly enhance the properties of state-of-the-art polymer-nanotube fibers.

*Author to whom correspondence should be addressed. Electronic address: M.Panhuis@hull.ac.uk

[1] D. A. Walters, L. M. Ericson, M. J. Casavant, J. Liu, D. T. Colbert, K. A. Smith, and R. E. Smalley, Appl. Phys. Lett. **74**, 3803 (1999).

[2] M.-F. Yu, B. S. Files, S. Arepalli, and R. S. Ruoff, Phys. Rev. Lett. **84**, 5552 (2000).

[3] A. B. Dalton, S. Collins, E. Munoz, J. M. Razal, V. H. Ebron, J. P. Ferraris, J. N. Coleman, B. G. Kim, and R. H. Baughman, Nature (London) **423**, 703 (2003).

[4] M. Cadek, J. N. Coleman, K. P. Ryan, V. Nicolosi, G. Bister, A. Fonseca, J. B. Nagy, K. Szostak, F. Béguin, and W. J. Blau, Nano Lett. **4**, 353 (2004).

[5] J. N. Coleman, M. Cadek, R. Blake, V. Nicolosi, K. P. Ryan, C. Belton, A. Fonseca, J. B. Nagy, Y. K. Gun'ko, and W. J. Blau, Adv. Funct. Mater. **14**, 791 (2004).

[6] J. N. Coleman, W. J. Blau, A. B. Dalton, E. Munoz, S. Collins, B. G. Kim, J. Razal, M. Selvidge, G. Viero, and R. H. Baughman, Appl. Phys. Lett. **82**, 1682 (2003).

[7] P. Nikolaev, M. J. Bronikowski, R. Kelley Bradley, F. Rohmund, D. T. Colbert, K. A. Smith, and R. E. Smalley, Chem. Phys. Lett. **313**, 91 (1999).

[8] G. Horvath and K. Kawazoe, J. Chem. Eng. Jpn. **16**, 470 (1983).

[9] E. P. Barret, L. G. Joyner, and P. H. Halenda, J. Am. Chem. Soc. **73**, 373 (1951).

[10] Pore diameter, $D_{\text{pore}} \sim [R^2\{4\sqrt{3}/\pi(1+d/R)-2/\pi\}+\sqrt{3}/\pi d^2]^{1/2}$, where R is the nanotube radius and d is the van der Waals distance.

[11] W. Zhou, Y. H. Ooi, R. Russo, P. Papanek, D. E. Luzzi, J. E. Fischer, M. J. Bronikowski, P. A. Willis, and R. E. Smalley, Chem. Phys. Lett. **350**, 6 (2001).

[12] S. Brunauer, P. H. Emmett, and E. Teller, J. Am. Chem. Soc. **60**, 309 (1938).

[13] S. M. Cooper, H. F. Chuang, M. Cinke, B. A. Cruden, and M. Meyyappan, Nano Lett. **3**, 189 (2003).

[14] P. W. Atkins, *Physical Chemistry* (Oxford University Press, New York, 1990).

[15] A. T. Fiory, S. Martin, L. F. Schneemeyer, R. M. Fleming, A. E. White, and J. V. Waszczak, Phys. Rev. B **38**, 7129 (1988).

[16] N. Vahdat and V. D. Sullivan, J. Appl. Polym. Sci. **79**, 1265 (2001).

[17] P. E. Rouse, J. Chem. Phys. **21**, 1272 (1953).

[18] M. Doi and S. F. Edwards, *The Theory of Polymer Dynamics* (Clarendon Press, Oxford, 1986).

[19] S. E. Lee and A. K. Chakraborty, J. Chem. Phys. **117**, 23 (2002).

[20] P. G. de Gennes, J. Chem. Phys. **55**, 572 (1971).

[21] In the intermediate case another mode characterized by entropic trapping may contribute; however, we will not consider this here; see J. Rousseau, G. Drouin, and G. W. Slater, Phys. Rev. Lett. **79**, 10 (1997).

[22] H. Krenchel, *Fibre Reinforcement* (Akedemisk Forlag, Copenhagen, 1964).

[23] W. D. Callister, *Materials Science and Engineering, an Introduction* (Wiley, New York, 2003).

[24] H. Pelzer, Rep. Prog. Phys. **6**, 330 (1939).

[25] S. F. Sun, *Physical Chemistry of Macromolecules* (Wiley, New York, 2004).

[26] Y. L. Li, I. A. Kinloch, and A. H. Windle, Science **304**, 276 (2004).

[27] M. Zhang, K. R. Atkinson, and R. H. Baughman, Science **306**, 1358 (2004).